Iranian Polymer Journal (2023) 32:1101–1110
https://doi.org/10.1007/s13726-023-01190-9

ORIGINAL RESEARCH

Computer simulation of the flow of a thermoplastic elastomer vulcanizate melt through an axisymmetric extrusion die using an augmented Navier's slip equation

Mir Hamid Reza Ghoreishy[1] · **Foroud Abbassi Sourki**[1]

Received: 25 February 2023 / Accepted: 7 May 2023 / Published online: 11 June 2023

Abstract

The pressure flows of a thermoplastic elastomer vulcanizate (TPV) melt through the die region of a single-screw extruder were simulated using the finite-element method. The COMSOL software was utilized to develop the finite-element model of the die and solve the working equations. ACross-WLF rheological equation of state was used for the description of the rheological behavior of the polymer melt. The numerical results were compared with their associated experimental data. The novel aspect of the present work is the development of a new augmented Navier's slip equation to take the effect of wall slip on solution variables into account. The proposed model consists of a power-law equation, which relates the slip coefficient to the shear rate at wall. It is implemented in the COMSOL code through a simple script. The distribution of the velocity, pressure, and temperature as well as the profile of the fluid velocity at exit region and slip velocity along the flow directions were presented and discussed. It has been shown that using the no-slip condition at wall or employing the Navier's slip equation with a constant slip coefficient leads to notable error in the prediction of mass flow rates and pressure.

✉ Mir Hamid Reza Ghoreishy
M.H.R.Ghoreishy@ippi.ac.ir

[1] Faculty of Processing, Department of Rubber Processing and Engineering, Iran Polymer and Petrochemical Institute, P. O. Box: 14975-112, Tehran, Iran

Graphical abstract

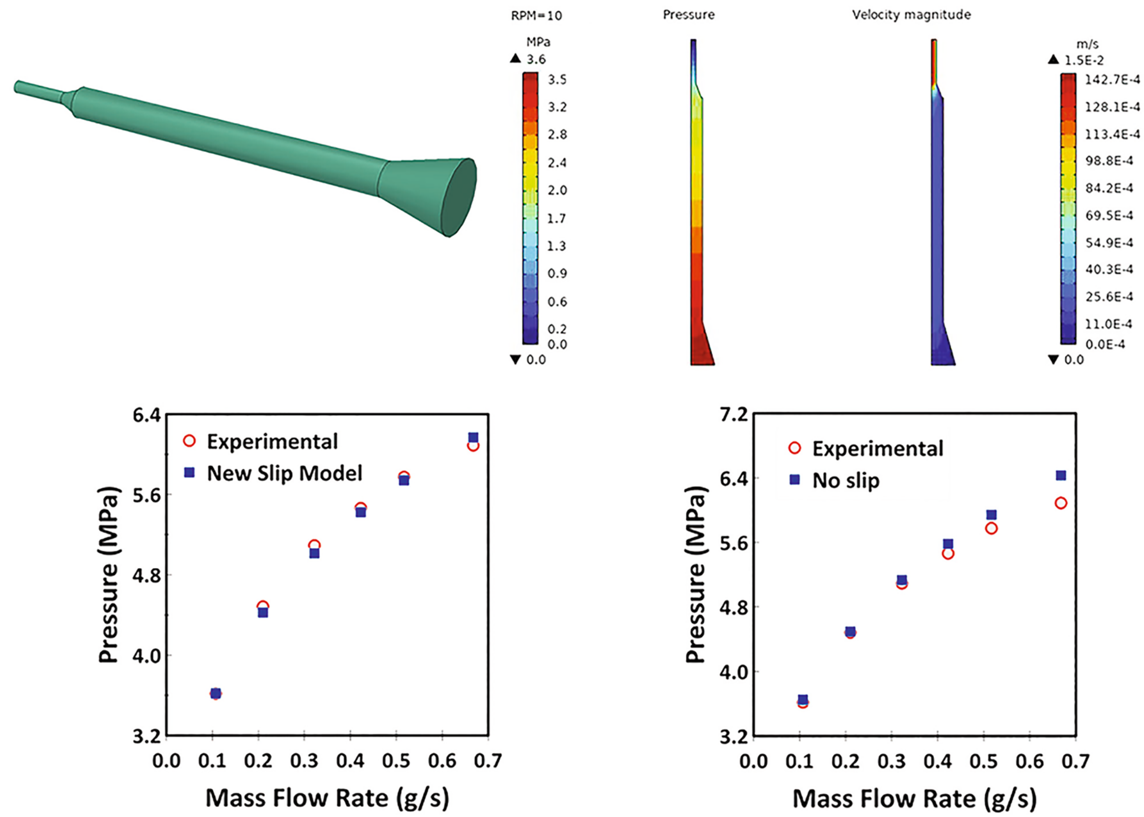

Keywords Simulation · Fluid flow · Polymer melt · COMSOL · Navier's slip

Introduction

It is generally known that extrusion is one of the fundamental processes that are extensively used for fabricating of polymers into products like rods, pipes, profiles, and sheets. In this process, the final form of the product is determined by flow of the polymer melt through a die. Therefore, a good understanding of the state of flow variables, such as velocity, pressure, and temperature, is vital to improve the die design, reduce the number of experimental trials and errors, and control of the flow. Dies are normally employed with an adapter (called a head) that connects to the exit region of the extruder barrel. The assembly of a die and head has usually complicated geometry, and thus, sophisticated mathematical models are required to fully describe the flow inside it. To achieve this task, numerical methods are commonly utilized in conjunction with commercial or in-house developed computer codes. In the past few decades, there has been a surge of interest in developing computer simulation techniques to analyze the flow of polymer melts through various domains, including extrusion dies. Several commercial softwares are available on the markets that are well suited for the modeling of the flow of non-Newtonian fluids in complex geometries. However, some polymeric fluids like rubbers and thermoplastic elastomers (TPEs/TPVs) present very high viscosity even at elevated temperatures. They also show viscoelastic nature, which means that their flow behaviors are between elastic solid and pure viscous materials. One of the consequences of these characteristics is the slip–stick phenomenon at the interface zone between polymer and solid walls, which makes the conventional no-slip assumption to be invalid. If the shear stress at the wall exceeds a critical value, there is a relative velocity between the fluid velocity at the wall and the wall velocity, which is called slip velocity. Traditionally, the slip of the melt at the solid wall is treated using a mathematical model known as Navier's slip equation [1–3]. This model suggests that the slip velocity is proportional to the shear stress at the wall. This equation is similar to the convection boundary condition in heat transfer (third type or Robin boundary condition). Navier's slip condition in a general three-dimensional framework is given by Eq. (1) [4]

$$-\frac{\eta}{\beta}\mathbf{S}.\left(\mathbf{u}-\mathbf{u}_{\mathrm{s}}\right)=\mathbf{S}.(\boldsymbol{\tau}.\mathbf{n}). \quad (1)$$

In this equation, $\mathbf{u}$ and $\mathbf{u}_s$ are the fluid and solid wall velocity vectors, respectively.$\boldsymbol{\tau}$ is the viscous stress tensor of the fluid, $\mathbf{n}$ is the unit vector normal to the plane in which the slip occurs, η is the shear viscosity, and β is a slip coefficient which is the momentum transfer coefficient at the interface between fluid and wall.$\mathbf{S}$ is a geometric tensor that projects vectors into the local tangent plane, expressed as

$$\mathbf{S} = \mathbf{I} - \mathbf{nn}. \tag{2}$$

$\mathbf{I}$ is the identity matrix. It has been shown that [5] for high viscous polymers when the wall slip is not taken into consideration, the predicted velocity profiles and the parameters derived from it such as flow rate have notable deviation from experimental data. Moreover, the original form of Navier's slip relationship is linear which fails to predict accurate results, especially at higher shear rates. Consequently, several modified and new relationships are proposed so far which are briefly reviewed in the background section. The present work is a re-visit of the use of Navier' slip condition during the modeling of a flow of a highly viscous non-Newtonian polymer melt (a commercial thermoplastic vulcanizate, TPV) through the die region of a single-screw extruder. A new relationship is introduced in which the slip coefficient is assumed to be related to the shear rate. It is shown that the suggested model gives rise to the prediction of more accurate results at higher screw speeds that correspond to high shear rates.

In the following sections, we first give a brief overview of the most important works published on the modeling of slip condition in fluid mechanics. We provide an account of the most recent findings and developments together with highlighting the novelty of our work. Then, the details of the governing equations, including the flow and energy, constitutive or rheological, and Navier's slip equations are presented. Following that, the developed finite-element models in this work are presented. Next, the experimental parts including the utilized die and extruder, rheological measurements techniques, and extrusion process are explained. The results and discussion are then presented in detail, and finally, conclusions are drawn.

Background

A considerable amount of literature has been published on the mathematical description of the slip phenomena during the flow of polymeric fluids in contact with solid walls. We, therefore, consider some of the works that are directly related to our selected approach. Lau and Schowalter [6] have developed a theoretical relationship for the slip velocity of an ethylene–propylene copolymer. Their model relates the slip velocity to the shear stress and temperature through a complex mathematical model given

$$v_s = C_1\left(\tau_w\right)^n\left[1 - C_2\tanh\left(\frac{E - C_3\tau_w}{kT}\right)\right], \tag{3}$$

where v_s is the slip velocity, τ_w is the shear stress at the wall, E is the activation energy, T is the temperature, and C_1, C_2, C_3, and k are the material constants. The model contains complex terms to consider the onset of the slip phenomenon or separation of the fluid at the wall. The basic idea of the work was on a combination of the concept of junctions at the wall/polymer interface as well as in the bulk of the polymer fluid with a kinetic equation describing a reaction, to which activation rate theory applies. Furthermore, an analogous slip velocity model was developed by Hatzikiriakos and Dealy [7]. Their model includes the first normal stress difference and molecular characteristic effects. They have experimentally studied the flow of a high-density polyethylene melt and determined the conditions for the onset of slip and the relationship between slip velocity and shear stress. Similar relationships were proposed by other researchers which are reviewed in a comprehensive literature survey by Hatzikiriakos [8]. In that work, it was stated that the slip happens macroscopically when the shear stress at the wall exceeds a critical value. Moreover, for linear polymers, a second critical shear stress is also observed in which a transition from weak to strong slip occurs. The focus of his work was, however, on the slip flow of molten polymers and no discussion was made for rubbery materials. Another complete review of slip phenomena including slip in polymer solutions, suspensions, and other complex fluids was also published by Archer [9]. The subjects of weak and strong slip were taken into consideration. Matthews and Hill [10] proposed a nonlinear Navier's slip model based on the work carried out by Thompson and Trojan [11]. They tested it for three simple pressure-driven flows using the Newtonian model without experimental verification. The main drawback with these models is the difficulty of imposing the developed equation into finite-element working equations and obtaining stable and convergent results. In addition, the applicability of the model for highly viscous rubbery materials has not been tested. Recently, Pérez-Salas et al. [12] developed a semi-analytic solution for the pressure flow of a Phan–Thien–Tanner fluid through an axisymmetric domain with Navier's slip condition at wall. They showed that the results of their model are in good accordance with those predicted by ANSYS Polyflow commercial code. Wilms et al. [13] studied the wall slip of non-Brownian suspensions in pressure-driven flows. They modified the classical equations by taking the effect of domain geometry on the slip into account.

From the practical point of view, there are also several published works in which computer simulations have been performed with different degrees of complexity to study the effects of wall slip on the flow variables. Ghoreishy and Nassehi [3] developed a finite-element code in which a novel method was introduced for the imposition of Navier's slip condition (Eq. 1). They have used their code for the simulation of the flow of rubbers in internal mixers. Later, Ghoreishy et al. [5] extended this code for the simulation of a TPE flow through the die region of a single extruder with axisymmetric geometry. They have shown that the ignoring slip wall leads to errors in the prediction of the flow rate. In the present research, we have proposed a work and an augmented form of Navier's slip condition for the numerical analysis of the flow of a highly viscous polymer melt through a die. Yang and Li [14, 15] considered the effect of wall slip for a CB/silica filled triple blend rubber (NR/SBR/BR) compound during oscillatory and steady shear rheometry. It was shown that the slip generally does not affect the oscillatory shear, but in the steady shear flow, it tends to make the measured shear viscosity to be lower than the actual value. Moreover, they have simulated the viscoelastic flow of the mentioned compound through an extrusion die by Polyflow software in which the wall slip was taken into consideration by a linear Navier's slip condition, given as

$$v_s = -\frac{\tau_w}{k}, \tag{4}$$

where k is the slip coefficient. Moreover, a 5-mode Phan–Thien–Tanner (PTT) model was also used as the rheological model. Having changed the slip coefficient, different profiles were predicted for the extrudate. It is reported that increasing the slip coefficient enlarges the predicted cross-sectional shape of the extrudate. Rippl [16] has used a power-law form for the slip velocity in an in-house developed finite-element code as

$$\tau_w = k_0 \left| v_s \right|^m. \tag{5}$$

They have simulated the flow of a rubber compound through a two-dimensional channel and three-dimensional die. The effects of three cases including no-slip, free wall slip (perfect slip), and partial slip on velocity and viscosity profiles were investigated. Mitsoulis et al. [17] studied the flow behavior of an SBR/CB rubber compound with a hardness of Shore A 70 in capillary and injection molding dies. They also considered the wall slip using a power-law temperature-dependent form similar to Eqs. (4) and (5) for slip velocity at walls. Both a pure viscous rheological model (Carreau) and a viscoelastic (K-KBZ) model were utilized in their simulations, which were carried out by their developed codes. They compared the predicted pressure drop with the experimental data and showed that accurate results can only be obtained by considering both viscoelasticity and wall slip. In summary, it can be deduced that due to the complex rheological behaviors of polymer melts, no single form for the slip velocity and its relation to shear stress at the wall can be used. In this work, we present a new form of slip coefficient in Navier's slip equation and verify it by comparing the results of the flow of a highly viscous polymer melt in an extruder die with their associated experimental data. Specifically, the novelty of our work is to propose a new form for the slip coefficient in Navier’s slip equation in which it is assumed that the slip coefficient is related to the shear rate through a power-law relationship.

Governing equations

The governing equations of the steady-state, non-isothermal, and laminar flow of an incompressible non-Newtonian fluid in an axisymmetric coordinate system (r, z) are given as follows [18]:

The equation of continuity:

$$\frac{\partial v_r}{\partial r} + \frac{v_r}{r} + \frac{\partial v_z}{\partial z} = 0. \tag{6}$$

The equation of motion in r-direction:

$$\rho\left(v_r\frac{\partial v_r}{\partial r} + v_z\frac{\partial v_r}{\partial z}\right) = -\frac{\partial p}{\partial r} + \frac{1}{r}\frac{\partial}{\partial r}\left(r\tau_{rr}\right) + \frac{\partial \tau_{zr}}{\partial z} - \frac{\tau_{\theta\theta}}{r} + \rho g_r. \tag{7}$$

The equation motion in z-direction:

$$\rho\left(v_r\frac{\partial v_z}{\partial r} + v_z\frac{\partial v_z}{\partial z}\right) = -\frac{\partial p}{\partial z} + \frac{1}{r}\frac{\partial}{\partial r}\left(r\tau_{rz}\right) + \frac{\partial \tau_{zz}}{\partial z} + \rho g_z. \tag{8}$$

The equation of energy:

$$\rho C_p\left(v_r\frac{\partial T}{\partial r} + v_z\frac{\partial T}{\partial z}\right) = \frac{1}{r}\frac{\partial}{\partial r}\left(rk\frac{\partial T}{\partial r}\right) + \frac{\partial}{\partial z}\left(k\frac{\partial T}{\partial z}\right) + \dot{S}. \tag{9}$$

In these equations, v_r and v_z are the components of velocity vector in r and z directions, respectively,ρ is the material density, p is the pressure, g_r and g_z are the components of the gravity vector, C_p is the specific heat, k is the thermal conductivity, T is the temperature, and $\dot{S}$ is the heat generated due to the viscous dissipation effect. The rheological behavior of the polymer melt is assumed to be described by the generalized Newtonian fluid as

$$\boldsymbol{\tau} = \eta\boldsymbol{\Delta}, \tag{10}$$

where $\boldsymbol{\tau}$ and $\boldsymbol{\Delta}$ are the viscous stress and rate-of-deformation tensors, respectively, expressed by the following relationships:

$$\boldsymbol{\tau} = \begin{bmatrix} \tau_{rr} & \tau_{rz} & 0 \\ \tau_{rz} & \tau_{zz} & 0 \\ 0 & 0 & \tau_{\theta\theta} \end{bmatrix} \tag{11}$$

$$\boldsymbol{\Delta} = \begin{bmatrix} 2\frac{\partial v_r}{\partial r} & \frac{\partial v_r}{\partial z} + \frac{\partial v_z}{\partial r} & 0 \\ \frac{\partial v_r}{\partial z} + \frac{\partial v_z}{\partial r} & 2\frac{\partial v_z}{\partial z} & 0 \\ 0 & 0 & 2\frac{v_r}{r} \end{bmatrix}. \tag{12}$$

Viscosity η (Eq. 10) in the present study is given by a modified Cross rheological model [19] expressed as

$$\eta = \eta_0 \left(1 + \left(\frac{\eta_0 \dot{\gamma}}{\tau_{cr}} \right)^{1-n} \right)^{-1}, \tag{13}$$

where n and τ_{cr} are two material constants. η_0 is dependent on temperature through the Williams-L and el-Ferry(WLF) equation given as

$$\eta_0 = D_1 e^{\left[\frac{-A_1 (T-T_c)}{A_2 + (T-T_c)}\right]}. \tag{14}$$

In this equation, A_1, A_2, and T_c are three material constants that should be determined by an appropriate experiment. In addition, $\dot{\gamma}$ is the shear rate which is related to the second invariant of the rate-of-deformation tensor by the following relationships:

$$\dot{\gamma} = \sqrt{\frac{1}{2} I_2} \tag{15}$$

$$I_2 = \left(2\frac{\partial v_r}{\partial r} \right)^2 + \left(2\frac{\partial v_z}{\partial z} \right)^2 + 2\left(\frac{\partial v_r}{\partial z} + \frac{\partial v_z}{\partial r} \right)^2 + \left(2\frac{v_r}{r} \right)^2. \tag{16}$$

Slip boundary condition

As stated previously, the slip of the polymer melt at the solid wall is considered by Navier's slip equation. The two-dimensional form of this equation (derived from Eq. 1) is given as

$$-\frac{\eta}{\beta} \mathbf{t}.\left(\mathbf{u} - \mathbf{u}_s \right) = \mathbf{nt} : \boldsymbol{\tau}, \tag{17}$$

where $\mathbf{t}$ is the unit vector tangent to the boundary. Additionally, as there is no penetration (cross-flow) at the wall, thus, the condition $\mathbf{u}.\mathbf{n} = 0$ should also be taken into consideration in conjunction with the above equation. Two forms for the slip coefficients β were considered. In the first form, a constant value has been assumed, while in the second form, which is also the novelty of this work, the following nonlinear equation has been proposed:

$$\beta = \beta_0 \dot{\gamma}^m, \tag{18}$$

where β_0 and m are two material constants. The details and justification of this new model will be given in the Results and discussion section.

Finite element model and flow simulation

The above-mentioned equations were solved using a finite-element model in an axisymmetric two-dimensional framework. The details of the working equations and solution algorithm can be found in the literature (for example [1]) and are therefore not repeated here. The COMSOL Multiphysics (laminar flow with heat transfer in fluids) v. 6.0 [20] was used for the simulation of flow in the die region. A mixed (also called u–v–p) finite-element method was used to solve the Navier–Stocks equations. A second-order discretization was used for the velocity, while a first-order one was employed for the pressure. The heat transfer was solved using the first-order discretization in conjunction with an upwinding technique to obtain stable results. The sketch of the flow domain is shown in Fig. 1. The flow domain was discretized into 99,279 triangular elements. An extra fine meshing size with controlled minimum and maximum element sizes was selected to achieve high-accuracy finite-element approximation. Figure 2 shows the selected mesh for different parts of the flow domain. Two series of simulations were carried out. In the first series, an input pressure was applied at the inlet of the domain (Fig. 1) and the associated flow field parameters, including the components of velocity vector, pressure, and temperature, were calculated as the primary variables. The mass flow rate was then calculated by integration of the velocity component (v_r) over the surface at the exit region. On the other hand, in the second series, a known value of the mass flow rate was assumed and the corresponding entry pressure was computed. It should be noted that, in each series, three different slip conditions including

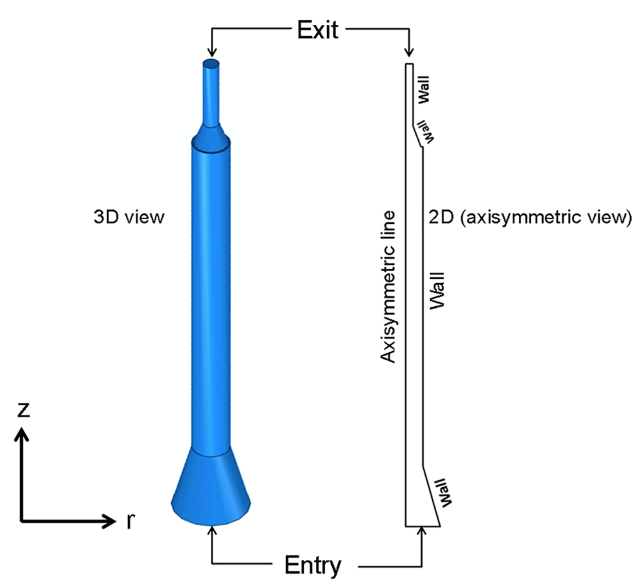

Fig. 1 Full shape of the die with the flow domain (axisymmetric coordinate system)

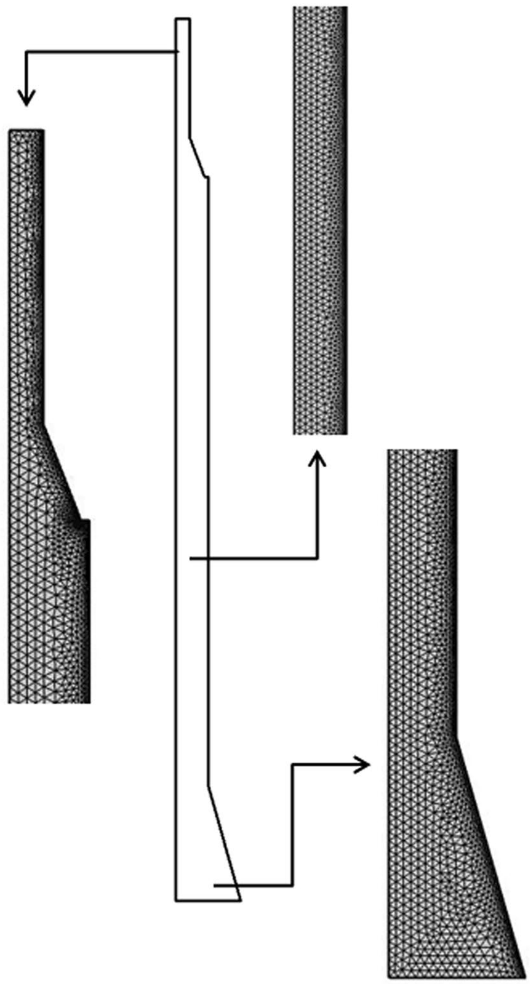

Fig. 2 Finite element mesh of the flow domain

no-slip ($\beta = 0$), linear Navier's slip equation ($\beta = constant$), and the proposed form of the Navier's slip equation (Eq. 18) were taken into account.

Experimental

To verify the developed model, the flow of a thermoplastic vulcanizate (TPV) through the die region of a laboratory single-screw extruder at different speeds was performed. The details of the materials and process are given below.

Materials

A commercial TPV (Elastron RD.121.A60.914) was selected in this work. It was a blend of PP (polypropylene) as the thermoplastic with a partially vulcanized EPDM as the elastomer parts. Density of the polymer was determined using an ADAM density measuring system. The specific heat and thermal conductivity were measured using Mettler Toldeo DSC and TCA200 (Taurus instrument), respectively. These physical and thermal properties are given in Table 1.

Table 1 Physical and thermal properties

Density-$\rho\left(\frac{Kg}{m^3}\right)$	Specific heat-$C_p\left(\frac{1}{kgK}\right)$	Thermal conductivity-$k\left(\frac{W}{mK}\right)$
920	2350	0.138

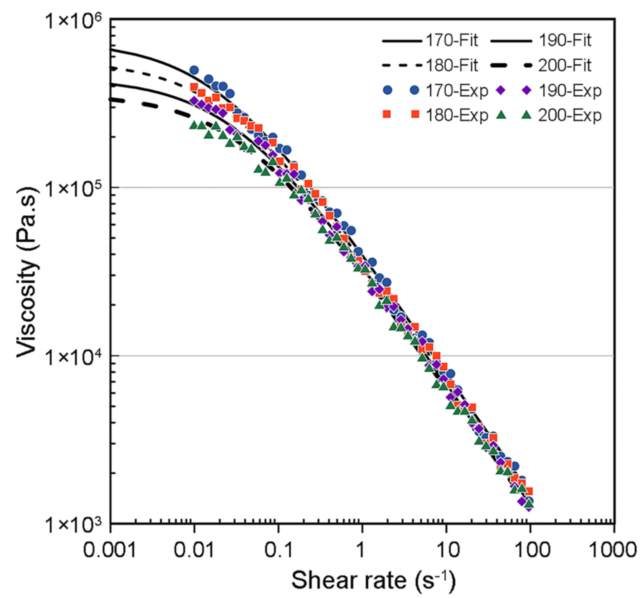

Fig. 3 Measured and fitted values of the viscosity versus shear rate at different temperatures

Table 2 Rheological properties (parameters of the equations)

$\tau_{cr}(Pa)$	n	$D_1(Pa.s)$	$A_1(K^{-1})$	$A_2(K)$	$T_c(K)$
13,500	0.28	3.2×10^{14}	11.26	52.5	275

Rheometry

The rheological behavior of the material was determined using a MCR501s, Anton Paar, Austria. The experiments were carried out in a shear rate sweep mode covering a range of 0.01–100 s^{-1}. A 25 mm parallel plate geometry with a gap of 2 mm, and various temperatures of 170–200 °C were applied. The Origin software v. 6.1 [21] was used to fit these data into the rheological Eqs. (13) and (14) by a nonlinear curve fitting technique. Figure 3 shows the variations of the experimentally measured and numerically fitted values of the viscosity versus shear rate at different temperatures. The predicted parameters are recorded in Table 2.

Extrusion process

The extrusion process of the selected TPV was carried out using a laboratory single-screw extruder equipped with a rod die, as shown in Fig. 1. Six screw speeds (10, 20, 30 40, 50, and 60 RPM) were selected. For each test run, the pressure at the entrance zone and the mass flow rate were measured. The temperatures of the die and the last zone of the barrel near the die were set at 190 °C.

Results and discussion

Simulations of the flow of the polymer melt were performed using the above-mentioned methods and process conditions. A uniform temperature of 190 °C was considered as the fluid entered the die. As it was pointed out in the previous sections, two series of simulations were carried out. In the first series, the pressure measured at the entrance zone was imposed as the boundary condition and the corresponding mass flow rates were computed, which are given in Fig. 4 with their associated experimentally measured data. Similarly, in the second series, the measured mass flow rates were considered as the boundary condition and the pressures at the inlet were computed, which have been compared with their experimental data, as depicted in Fig. 5. In both cases, the no-slip boundary conditions were applied at the wall. Comparing the results in each series, it can be seen that increasing the entry pressure or assuming a higher mass flow rate gives rise to an increase in the deviation of the computed values from their experimental counterparts. This result supports our previous assumption [5] that ignoring the wall slip, especially at higher shear rates leads to the computation of a lower value for mass flow rate than the experimentally measured value. The distributions of the computed temperatures are shown in Fig S1a–f in the Supplementary Materials. It is worth noting that the maximum difference between inlet and outlet temperatures is within 3 °C, which means that although a non-isothermal analysis is performed in this work, an almost isothermal condition is obtained. Consequently, the remaining finite-element analyses have been carried out based on an isothermal assumption. Moreover, Fig S2a-f in the Supplementary Materials show the computed pressure and velocity fields inside the flow domain for different entry pressures corresponding to the selected six screw speeds. As it can be seen and expected, the pressure gradually decreases along the flow direction from its maximum value (entry pressure) to nearly zero at the exit region, which confirms the existence of a typical and classic pressure flow. In addition, the velocity field shows that by decreasing the cross-section area of the die in z-direction, the velocity vector increases.

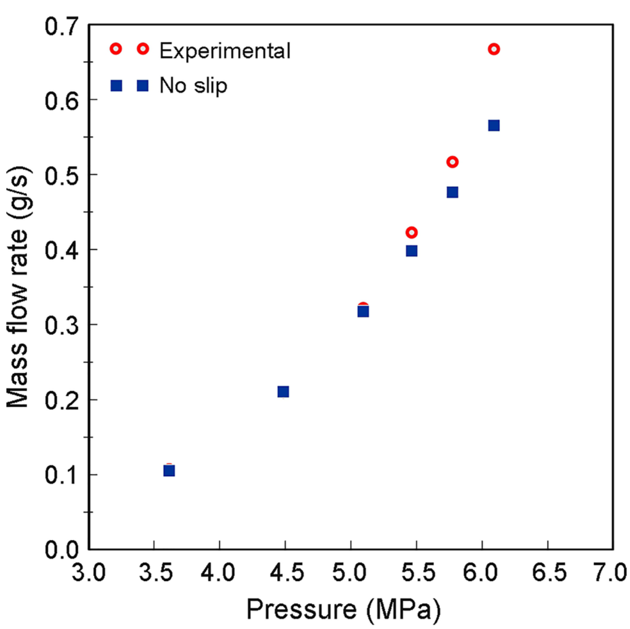

Fig. 4 Computed mass flow rate versus entry pressure with no-slip boundary condition

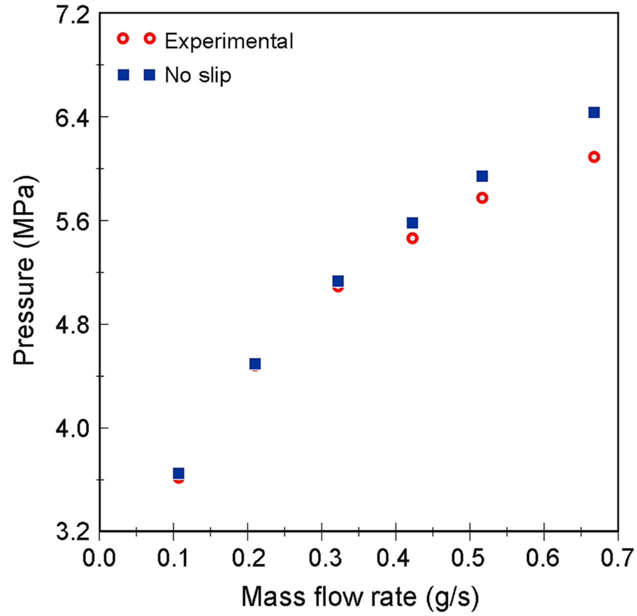

Fig. 5 Computed entry pressure versus mass flow rate with no-slip boundary condition

To study the effect of the wall slip on the results, the increase in observation in the difference between predicted and experimental values (pressure and mass flow rate) could be attributed to the lower average velocity with the no-slip condition. In fact, with increasing the entry pressure (or mass flow rate), the boundary layer diminishes, leading to the generation of a higher component of the velocity along the flow direction. To further verify and quantify this

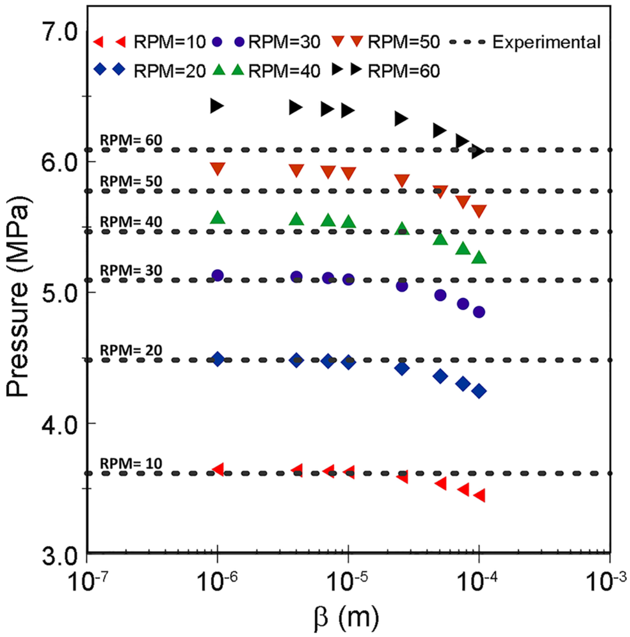

Fig. 6 Computed entry pressure versus experimental data at different slip coefficients

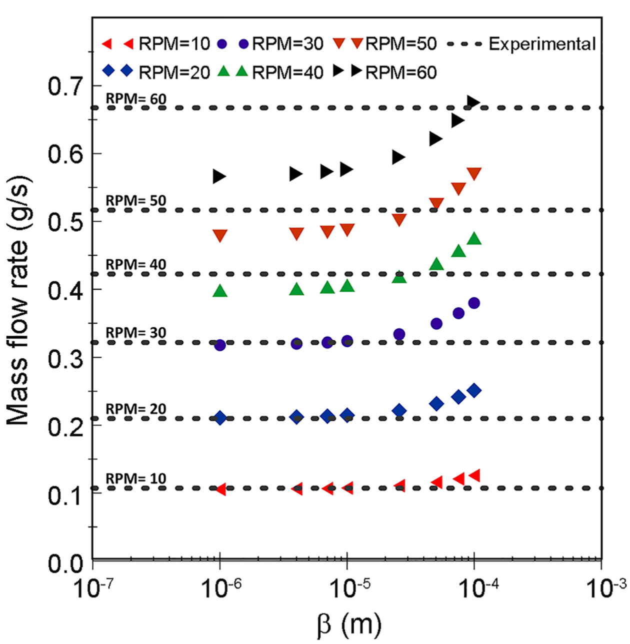

Fig. 7 Computed mass flow rate versus experimental data at different slip coefficients

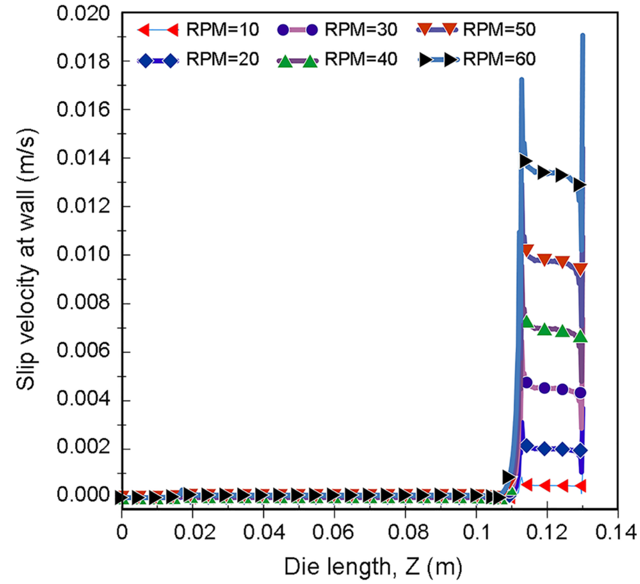

Fig. 8 Slip velocity along flow direction at different screw speeds

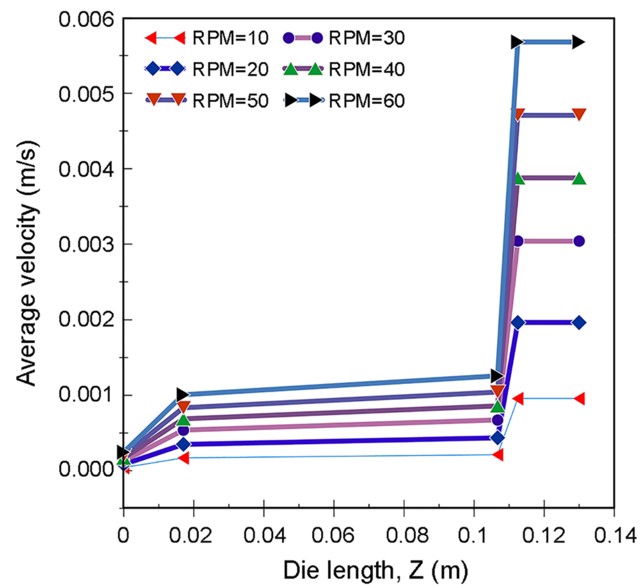

Fig. 9 Average velocity along flow direction at different screw speeds

statement, the simulations were repeated with Navier's slip wall condition with different values for slip coefficients (β). The computed entry pressure and mass flow rates against different slip coefficients are plotted and shown in Figs. 6 and 7, respectively. The presented computational results in these graphs are also compared with experimental data. As it can be seen, the discrepancy between the predicted entry pressure and mass flow rates with experimental data decreases with increasing of the slip coefficient (β). In addition, the profile of the computed slip velocity and average velocity along the flow direction are shown in.

Figures 8 and 9, respectively. As it can be seen, there is a significant increase in slip velocity when the polymer melt enters the final section, which is also the narrowest part of the die. It should be pointed out that the jumps in the velocity profiles at two points at the entry and exit region of the final section are due to the singular points at these regions and attributed to the numerical instabilities created. To further consider this point, the distributions of the shear rates for these simulations are plotted as shown in Fig. S3a–f in the Supplementary Materials. It is apparent from these figures that by increasing the entry pressure, the shear rates significantly increase (as expected) especially at the narrowest section. Therefore, we may conclude that there should be a direct relation between slip coefficient and shear rate, which could be attributed to the complicated interactions between polymer melt and the inner surface of the die. This reveals the need for a new format for the slip coefficient, which is related to the state of rate-of-deformation. Consequently, we have assumed in the present work that the slip coefficient (β) can be related to the shear rate by a power-law relationship as given in Eq. (18). To find the parameters for this equation, the best value of the slip coefficient for each entry, as shown in Figs. 6 and 7, was chosen in conjunction with its associated average value of the shear rate at the exit zone. It should be explained that, as it can be seen in Fig. 8, the slip velocity at the final zone of the die is much higher than its corresponding value at the other zones. Therefore, the average value of the shear rate was calculated at the exit region. Using a simple curve fitting approach, the values of β_0 and m in this equation are found and given in Table 3.

The associated variations of the computed mass flow rate versus experimentally determined entry pressure and computed entry pressure versus experimentally measured mass flow rates are shown in Figs. 10 and 11, respectively. It can be seen that, by assuming a variable slip coefficient, very close agreements are obtained between the computed variable and experimental data which confirms our assumption and the proposed model.

The distributions of the pressure and velocity for the flow with variable slip coefficient are shown in Fig. S4a–f in the Supplementary Materials. Compared with their corresponding distributions (no-slip boundary conditions) as shown in Fig S2a–f) in the Supplementary Materials, it can be seen that there are slight differences between the predicted pressure and velocity between two series of simulations. To further study the effect of the wall boundary conditions, the velocity profile at the exit region, with and without slip at wall for the six screw speeds, is plotted and shown in Fig S5a–f in the Supplementary Materials, respectively. Here, it can be seen that the velocity profile for the no-slip case is lower than the computed velocity variations when the wall slip is taken into account. This is the reason that the computed mass flow rates for no-slip boundary conditions are lower than in the case

Table 3 Computed parameters of Eq. (18)

$\beta_0 (m.s^m)$	m
5×10^{-7}	1.1

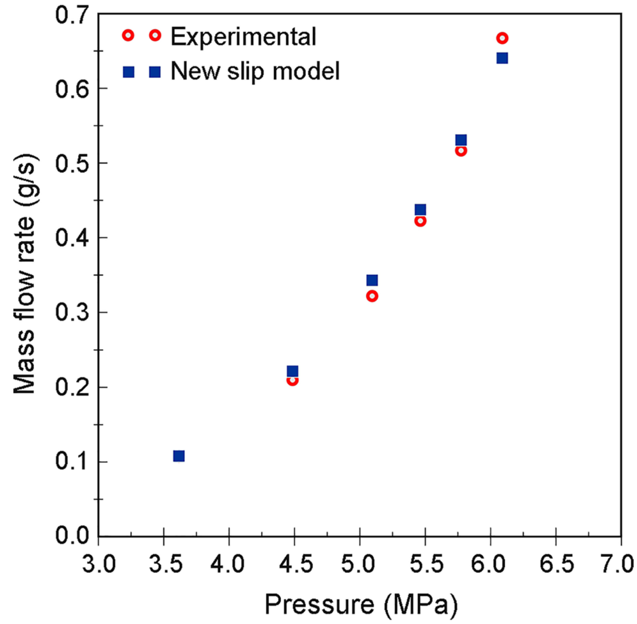

Fig. 10 Computed mass flow rate versus entry pressure with modified Navier's slip equation

where the slip condition is imposed into the working equations. Besides, as expected, by increasing the screw speed (or entry pressure), the difference between velocity profiles, with and without wall slip conditions, becomes more prominent, which is in agreement with our previous finding.

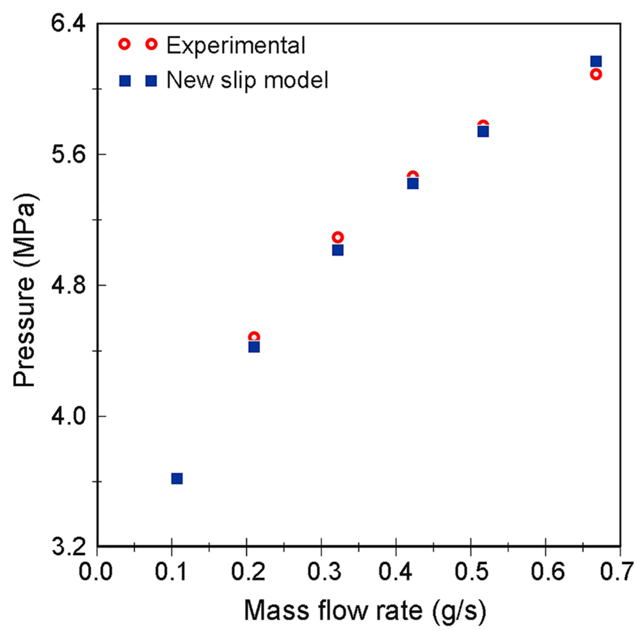

Fig. 11 Computed pressure versus mass flow rate with modified Navier's slip equation

Conclusion

The flow of a polymer melt with a generalized Newtonian temperature-dependent rheological model through the die of a single-screw extruder was simulated using the COMSOL software. Different slip conditions at solid walls including the no-slip, Navier's slip equation with constant coefficient and a newly proposed model based on Navier's slip equation with variable coefficient were considered. It has been shown that due to the complex interaction between polymer melt and the inner surface of the wall, the assumption of a constant slip coefficient is not valid. Consequently, we have proposed a new phenomenological form in which the slip coefficient is related to the shear rate at wall by a power-law model. Having compared mass flow rate and entry pressure computed from the simulation results with their corresponding experimentally measured data, the applicability and accuracy of this new model was proved. It is recommended that further research should be undertaken to assess the proposed model for three-dimensional problems and check its validity for more complicated frameworks.

Supplementary Information The online version contains supplementary material available at https://doi.org/10.1007/s13726-023-01190-9.

Acknowledgements The authors would like to acknowledge the Iran Polymer and Petrochemical Institute for permission to publish the results presented in this paper.

Data availability Data sets generated during the current study are available from the corresponding author on reasonable request.

References

1. Nassehi V (2002) Practical Aspects of Finite Element Modelling of Polymer Processing, 1st edn. Wiley
2. Nassehi V, Ghoreishy MHR (1997) Simulation of free surface flow in partially filled internal mixers. Int Polym Process 12:346–353
3. Ghoreishy MHR, Nassehi V (1997) Modeling the transient flow of rubber compounds in the dispersive section of an internal mixer with slip-stick boundary conditions. Adv Polym Technol J Polym Process Inst 16:45–68
4. Silliman WJ, Scriven LE (1980) Separating flow near a static contact line: slip at a wall and shape of a free surface. J Comput Phys 34:287–313
5. Ghoreishy MHR, Razavi-Nouri M, Naderi G (2000) Finite element analysis of flow of thermoplastic elastomer melt through axisymmetric die with slip boundary condition. Plast Rubber Compos 29:224–228
6. Lau HC, Schowalter WR (1986) A model for adhesive failure of viscoelastic fluids during flow. J Rheol 30:193–206
7. Hatzikiriakos SG, Dealy JM (1991) Wall slip of molten high-density polyethylene. I. Sliding plate rheometer studies. J Rheol 35:497–523
8. Hatzikiriakos SG (2012) Wall slip of molten polymers. Prog Polym Sci 37:624–643
9. Archer LA (2005) In: Hatzikiriakos SG, Migler KB (Eds) Polymer Processing Instabilities, Control and Understanding. Marcel &Dekker, New York
10. Matthews MT, Hill JM (2007) Newtonian flow with nonlinear Navier boundary condition. Acta Mech 191:195–217
11. Thompson PA, Troian SM (1997) A general boundary condition for liquid flow at solid surfaces. Nature 389:360–362
12. Pérez-Salas KY, Ascanio G, Ruiz-Huerta L, Aguayo JP (2021) Approximate analytical solution for the flow of a Phan-Thien–Tanner fluid through an axisymmetric hyperbolic contraction with slip boundary condition. Phys Fluids 33:053110
13. Wilms P, Wieringa J, Blijdenstein T, van Malssen K, Hinrichs J, Kohlus R (2020) Wall slip of highly concentrated non-Brownian suspensions in pressure driven flows: A geometrical dependency put into a non-Newtonian perspective. J Non-Newton Fluid Mech 282:104336
14. Yang C, Li Z (2014) A study of wall slip in the capillary flow of a filled rubber compound. Polym Test 37:45–50
15. Yang C, Li Z (2016) Effects of wall slip on the rheological measurement and extrusion die design of a filled rubber compound. Plast Rubber Compos 45:326–331
16. Rippl AP (2004) Three-dimensional simulation of rubber profile extrusion on the basis of in-line rheometry. Swansea University (United Kingdom)
17. Mitsoulis E, Battisti M, Neunhäuserer A, Perko L, Friesenbichler W, Ansari M, Hatzikiriakos SG (2017) Flow behaviour of rubber in capillary and injection moulding dies. Plast Rubber Compos 46:110–118
18. Bird RB, Stewart WE, Lightfoot EN (2006) Transport Phenomena, 2nd edn. John Wiley, Inc
19. Shi XZ, Huang M, Zhao ZF, Shen CY (2011) Nonlinear fitting technology of 7-parameter cross-WLFviscosity model. In: Advanced Materials Research. Trans Tech Publ 2011:2103–2106
20. COMSOL Multiphysics, Ver. 6.0, COMSOL Inc.,
21. Origin software, Ver. 6.1, 2000